direction. However, a tilt range of 10° would cover 17.4 % of reciprocal space, and if it is possible to collect high quality diffraction data up to 1Å resolution, this would still be much more than 1 independent reflection per non-hydrogen atom.

In contrast to precession electron diffraction (PED) [5] LARBED includes all tilt angles within the limits of the tilt range and thus records diffraction intensities at the Bragg condition for a large range of diffraction conditions. Averaging over all these different Umweg excitations allows one to reconstruct quasi-kinematic diffraction intensities for part of 3D reciprocal space, as shown in Figure 1 for the example of $K_2O{\cdot}7Nb_2O_5$ [6], in a random [hk0] orientation. $K_2O{\cdot}7Nb_2O_5$ has space group P4/mbm (No. 127) and unit cell vectors of length a = b = 27.5Å and c = 3.94 Å. The data was automatically acquired using the QED DM-PlugIn by HREM Research [7].

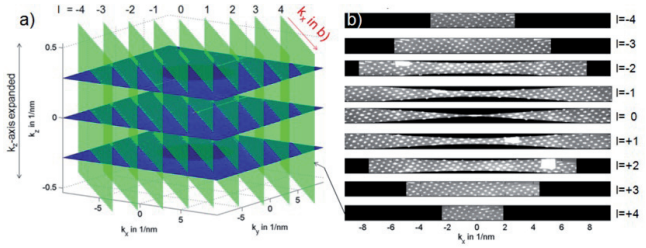

Figure 1: a) 3D reciprocal space reconstructed from the data shown in Fig. 2. Because of the tilt range of only ± 4° the missing wedge is rather large. The vertical component spans a range of -0.5 $nm^{-1} \leq k_z \leq 0.5$ nm^{-1}. The green slices correspond to the vertical cuts through this 3D space shown in b). b) Positions of diffraction spots in 3D reciprocal space at different parallel planes. The intensities are the mean intensities averaged over a large number of diffraction patterns for which the Ewald sphere cut through that voxel in k-space. The contrast has been adjusted to reveal all reflections, not just the very bright ones. (White areas are due to the CCD read-out streak of very intense peaks.)

[1] C.T. Koch, P. Bellina, P.A. van Aken, *EMC 14, vol. 2: Materials Science*, Springer, Berlin Heidelberg, **2008**, 201–202. [2] C.T. Koch, *Ultramicroscopy* **2011**, *111*, doi:10.1016/j.ultramic.2010.12.014. [3] U. Kolb, T. Gorelik, C. Kübel, M.T. Otten, D. Hubert, *Ultramicroscopy* **2007**, *107*, 507–513. [4] D. Zhang, P. Oleynikov, S. Hovmöller, X. Zou, *Z. Kristallogr.* **2010**, *225*, 94–102. [5] R. Vincent, P.A. Midgley, *Ultramicroscopy* **1994,** *53*, 271–282. [6] D Zhang et al., *Ultramicroscopy* **2010,** *111*, 47–55. [7] http://www.hremresearch.com/Eng/plugin/QEDEng.html

Keywords: 3D electron diffraction, precession electron diffraction, aberration correction

MS79.P12

Acta Cryst. (2011) A**67,** C697

Structure analysis of charge-orbital ordered phases in *A*-site ordered $SmBaMn_2O_6$ using CBED

Daisuke Morikawa,[a] Kenji Tsuda,[a] Shigeki Yamada,[b] Takahisa Arima,[a,c] [a]*IMRAM, Tohoku Univ., (Japan).* [b]*Inter. Grad. Sch. Arts and Sci., Yokohama City Univ., (Japan).* [c]*Dept. Adv. Mat. Sci., Univ. Tokyo, (Japan).* E-mail: morikawa@mail.tagen.tohoku.ac.jp

A structure analysis method using convergent-beam electron diffraction (CBED) developed by Tsuda and Tanaka [1] enables us to directly determine crystal structures and electrostatic potential distributions from nanometer-scale specimen areas. Using the method, sp^3 bonding electrons of silicon [2] and an ordered state of Fe 3*d* $3z^2$-r^2 orbitals of spinel oxide $FeCr_2O_4$ [3] were successfully observed. In the present study, the CBED method has been applied to an *A*-site ordered perovskite-type oxide $SmBaMn_2O_6$. The *A*-site ordered $SmBaMn_2O_6$ contains the alternate stack of SmO and BaO sheets along the *c*-axis with intervening MnO_2 sheets. This material undergoes a structural phase transformation at 190 K from a room temperature (RT) phase with charge- and orbital-ordering (COO) to a low-temperature (LT) COO phase [4]. Some different COO models have been proposed for the RT and LT phases. We aim to determine the crystal structures and COO patterns of the RT and LT phases and examine the relations between microscopic crystal structures and macroscopic physical properties. It is noted that the influence of the *A*-site randomness on CBED patterns can be excluded unlike the *A*-site disordered phase.

CBED patterns of $SmBaMn_2O_6$ were obtained at 293 K and 90 K using an energy-filter transmission electron microscope JEM-2010FEF operated at an accelerating voltage of 100 kV. The space groups of the RT and LT phases were determined by the CBED method. Based on the determined space groups, atom positions, atomic displacement parameters and low-order structure factors were refined by nonlinear least square fitting between the CBED patterns and dynamical diffraction calculations using our analysis software MBFIT [1].

From the symmetries of CBED patterns taken with five different incidences, the point group of the RT phase was determined to be *mmm*. The lattice type was determined to be primitive because no extinction by lattice type was observed. Dynamical extinction lines (DELs) were seen in the *h*00 (*h*=odd) zeroth-order Laue zone (ZOLZ) reflections and 0*kl* (*k*+*l*=2n+1) higher-order Laue zone (HOLZ) reflections, which indicate the existence of an *a*-glide symmetry perpendicular to the *b*-axis and an *n*-glide symmetry perpendicular to the *a*-axis, respectively. Thus, the space group of the RT phase of $SmBaMn_2O_6$ was uniquely determined to be *Pnam* (No. 62). There are two different models were reported for the RT-COO phase. From the space group, an allowed COO model was selected.

Similarly, the space group of the LT phase was also determined to be *Pmam* (No. 51) and a possible COO model was also selected.

The result of the refinement of crystal structural parameters will be presented.

[1] K. Tsuda, M. Tanaka, *Acta Cryst.***1999,** *A55*, 939. [2] Y. Ogata *et al.*, *Acta. Cryst.* **2008,** *A64*, 587. [3] K. Tsuda *et al*., *Phys. Rev.* **2010,** *B81*, 180102. [4] D. Akahoshi *et al*., *Phys. Rev. B70*, **2004,** 064418.

Keywords: convergent_beam_electron_ddiffraction, TEM, charge_orbital_ordering

MS79.P13

Acta Cryst. (2011) A**67,** C697-C698

Electric field induced deformation in piezoelectric LiH_2PO_4 and LiH_2PO_3 crystals

M. Al Taani,[a] S. Wagner,[a] O. Schmidt,[a] U. Pietsch,[a] C. Lehmann,[b] [a]*Solid State Physics Department, University of Siegen, Siegen, (Germany).* [b]*Max-Planck-Institute of Kohlenforschung, Muelheim, (Germany).* E-mail: altaani@deph.physik.uni-siegen.de

LiH_2PO_4 and LiH_2PO_3 crystallize in space group symmetry $Pna2_1$ and show piezoelectric properties. Single crystalline plates have been investigated under external high-electric field to study structural changes due to the internal deformation. The experiments have been performed using a four-circle diffractometer at D3 beamline @ DESY in ω scan mode combined with an open X-ray point detector. Diffraction curves of LiH_2PO_4 crystal (a_1=6.253, a_2=7.656, a_3=6.881, Z=4)[1]with orientations [011] and [201] were under an external electric field (±3 kV mm^{-1}). The measured peaks shifts reproduce the piezoelectric constants d_{ijk} of the material, the internal changes of atomic positions are deduced from changes of integrated intensities. The internal deformation was calculated to be larger for the Li-O bond compared to that of the P-O bonds. Normalized to an applied electric

field E = 1 kV mm^{-1}, the changes of bond length were $(5.2\pm0.2)10^{-5}$ Å and $(3.0\pm0.8)10^{-5}$ Å, respectively. The same measurements on LiH_2PO_3 (a_1=11.024, a_2=5.060, a_3=5.169, Z=4)[1]are under way and will be compared with the results of LiH_2PO_4. This will help to understand the relationship between external deformation and the specific response of chemical bonds in ternary compounds.

[1] S. Haussühl, *Cryst. Res. Technol. 31,* **1996**, 323-327.

Keywords: piezoelectric, deformation, electric field.

MS79.P14

Acta Cryst. (2011) A**67,** C698

Crystallographic analysis of $xLi_2MnO_3\cdot(1-x)LiMO_2$ material for lithium batteries.

LubaBurlaka,[a] Judith Grinblat,[a] Francis Amalraj,[b] Michael Talianker,[b] Boris Markovsky,[b]Doron Aurbach,[a,b]. [a]*Bar-Ilan Institute of Nanotechnology and Advanced Materials, Bar-Ilan University, Ramat-Gan.* [b]*Department of Chemistry, Bar-IlanUniversity, Ramat-Gan (Israel).* E-mail: luba@nano.biu.ac.il

In recent years layered compounds of the $xLi_2MnO_3\cdot(1-x)Li(TM)O_2$ series (TM = transition metal or a combination of transition metals with Mn x=0.3; 0.5; 0.7) have been extensively studied as promising cathode materials for lithium-ion batteries. The $Li(TM)O_2$ structural component adopts a layered α-$NaFeO_2$-type structure (rhombohedral R-3m symmetry) in which the Na sites are occupied by Li, and the Fe sites are occupied by TM ions, thus forming alternating lithium layers and layers of transition metal separated by close-packed oxygen atomic planes. During the charge/discharge cycle, Li ions leave/fill theirsites, while charge neutrality of the unit cell is preserved by oxidation/ reduction of TM atoms. The second component, Li_2MnO_3 (monoclinic, *C2/m*), is also associated with the parent layered structure of α-$NaFeO_2$: like in the rhombohedral $Li(TM)O_2$ phase Li and Mn atoms occupy, respectively, Na and Fe sites in the α-$NaFeO_2$-type structure, however excess Li atoms substitute for Mn at 1/3 of the atomic positions in Mn-planes.

The Li_2MnO_3 compound is normally electrochemically inactive for lithiuminsertion and extraction,however, when synthesized in a nanocrystalline form it becomes electroactivite, probably due to the factors associated with the material's defectchemistry, which is not well understood. Moreover, there is a subject for discussions in the literature whether the compounds $xLi_2MnO_3\cdot(1-x)Li(TM)O_2$form homogeneous solidsolutionsor contain Li_2MnO_3 domains within a $Li(TM)O_2$matrix. Thus, crystallographic structural studies of Li_2MnO_3 are both of fundamental and technologicalinterest.

In this study, we present our results of investigation of the structure of $xLi_2MnO_3\cdot(1-x)Li(Mn1/3Ni1/3Co1/3)O_2$ material by XRD, electron diffraction and high-resolution transmission electron microscopy techniques. The material was synthesized by a self-combustion reaction (SCR) using precursors of lithium nitrate, nickel (II) nitrate, manganese (II) nitrate, and cobalt (II) nitrate as oxidants and sucrose as the fuel.

On the basis of results Rietveld analysis of powder XRD patterns it was concluded that structure of this material consists of two components: the rhombohedral phase possessing the structure of $LiNiO_2$ (space group *R-3m*) and the monoclinic phase Li_2MnO_3 described by space group *C2/m*. Varying the ratios of the Ni, Co and Mn occupancies on the nickel site in the $LiNiO_2$ structure and varying Mn occupancy and Li/Mn ratio in sites *4g* and *2b*, respectively, in the Li_2MnO_3 structure we obtained that in the $LiNiO_2$ phase the lithium occupancy on the *3b* site is 100 %. Hence, the lithium layer is not contaminated, and the Li/Mn ratio on the *2b* in Li_2MnO_3 phase is about 5/4.

TEM examinations of $xLi_2MnO_3\cdot(1-x)LiMn1/3Ni1/3Co1/3O_2$ provided evidence that the material is comprised of nanodomains of both rhombohedral $LiNiO_2$-like and monoclinic Li_2MnO_3 structures, which are integrated and interconnected with one another at the atomic level. It was possible to distinguish between both componentsin high resolution micrographs.

Keywords: structural characteristics, TEM, cathode materials

MS80.P01

Acta Cryst. (2011) A**67,** C698-C699

Dynamic control of photochromic property in Salicylideneaniline hydrate crystals

Kohei Johmoto, Akiko Sekine, Hidehiro Uekusa, *Department of Chemistry and Materials Science, Tokyo Institute of Technology, (Japan).* E-mail: johmoto@chem.titech.ac.jp

Photochromism, light-induced reversible color change of substances, has attracted much attention due to its potential applications such as optical data storages, rewritable paper and biomolecular sensor etc. Salicylideneaniline (SA) derivatives are well-known solid-state photochromic substances that change the color from yellow to red by UV irradiation and red to yellow by visible light irradiation or heat. The yellow to red color change is explained as a tautomerism from the enol (yellow) to the cis-keto intermediate form followed by conformational change to the trans-keto form (red), which is cis-trans isomerization. In this study, we introduce the dynamic control of the photochromic property in SA hydrate crystals using hydration and dehydration process.

As a part of photochromic property control study by modifying molecular conformation and crystal environment[1], some hydrated crystals were obtained. The crystal of *N*-salicylidene-4-carboxyaniline was a photochromic hemihydrate phase (**1a**). After heating, it was found that the hydrated phase has changed to a new dehydrated phase without photochromic property. In the crystal structure of the hydrated phase, the molecular structure of SA moiety had a non-planar conformation, the intra-molecular dihedral angle was 45 degrees. This result is in agreement with the knowledge that the non-planar SA derivative has a photochromic property. From these results, it is supposed that the dehydration process (pseudo-polymorphic transition) causes the conformational change from non-planar to planar of SA molecule due to the crystalline environment changes.

Meanwhile the co-crystal of *N*-salicylidene-3-carboxyaniline and 4-acetamidepyridine was obtained as a monohydrate crystalline phase (**2a**) showing no photochromism. However, under low-humidity condition or by heating, it transformed into new photochromic crystalline phase (**2b**) which was analyzed to be dehydrated. Reversibly this dehydrated phase (**2b**) turned to monohydrate phase (**2a**) by water vapor application and the photochromic property disappeared. This photochromism switching is explained by the change of intra-molecular dihedral angles in phases **2a** (27degrees, non-photochromic) and **2b** (43degrees, photochromic).

These results show that the photochromic property of SA is dynamically controlled by crystalline environmental change due to the hydration / dehydration processes and additionally in the **2a** and **2b** phases the photochromism switching property was realized.

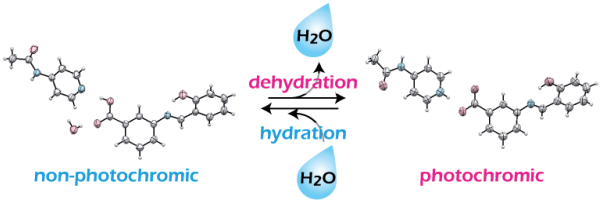

Photochromism switching by hydration and dehydration processes